Published in final edited form as:
Clin Cancer Res. 2014 June 1; 20(11): 2922–2932. doi:10.1158/1078-0432.CCR-13-1246.

Zoledronic acid has differential anti-tumour activity in the pre- and post-menopausal bone microenvironment *in vivo*

Penelope D Ottewell[1], **Ning Wang**[2], **Hannah K Brown**[1], **Kimberly J Reeves**[2], **C Anne Fowles**[2], **Peter I Croucher**[3], **Colby L Eaton**[2], and **Ingunn Holen**[1]

[1]Academic Unit of Clinical Oncology, Department of Oncology, University of Sheffield, S10 2RX, UK

[2]Bone Biology, Department of Human Metabolism, University of Sheffield, S10 2RX, UK

[3]Musculoskeletal Medicine Division, Garvan Institute of Medical Research, Sidney, New South Wales, Australia

Abstract

Purpose—Clinical trials in early breast cancer have suggested that benefits of adjuvant bone targeted treatments are restricted to women with established menopause. We developed models that mimic pre- and post-menopausal status to investigate effects of altered bone turnover on growth of disseminated breast tumour cells. Here we report a differential anti-tumour effect of zoledronic acid (ZOL) in these two settings.

Experimental design—12-week old female Balb/c-nude mice with disseminated MDA-MB-231 breast tumour cells in bone underwent sham operation or ovariectomy (OVX), mimicking the pre- and post-menopausal bone microenvironment, respectively. To determine the effects of bone-targeted therapy, sham/OVX animals received saline or 100ug/kg ZOL weekly. Tumour growth was assessed by i*n vivo* imaging and effects on bone by RT-PCR, microCT, histomorphometry and measurements of bone markers. Disseminated tumour cells were detected by two-photon microscopy.

Results—OVX increased bone resorption and induced growth of disseminated tumour cells in bone. Tumours were detected in 83% of animals following OVX (post-menopausal model) compared to 17% following sham operation (pre-menopausal model). OVX had no effect on tumours outside of bone. OVX-induced tumour growth was completely prevented by ZOL, despite the presence of disseminated tumour cells. ZOL did not affect tumour growth in bone in the sham-operated animals. ZOL increased bone volume in both groups.

Conclusions—This is the first demonstration that tumour growth is driven by osteoclast-mediated mechanisms in models that mimic post-but not pre-menopausal bone, providing a biological rationale for the differential anti-tumour effects of ZOL reported in these settings.

Corresponding author: Dr. Penelope Ottewell, Academic Unit of Clinical Oncology, Medical School, University of Sheffield, Beech Hill Road, Sheffield, S10 2RX, UK., Telephone: +44 (0) 114 271 2133, Fax: +44 (0) 114 271 1711, P.D.Ottewell@sheffield.ac.uk.

Conflicts of interest: Authors have no conflicts of interest to declare.

Europe PMC Funders Author Manuscripts

Keywords

Breast cancer; ménopause; zoledronic acid; mouse models

Europe PMC Funders Author Manuscripts

Introduction

There is increasing evidence of differential therapeutic effects of bone-sparing agents in the pre- and post-menopausal setting from clinical trials in breast cancer, with benefits largely confined to women with established menopause (1-3). These results indicate that the mechanisms that govern breast cancer progression, and also the response to therapeutic intervention, are influenced by the endocrine status of the patient. The first indication that menopausal status was important in determining the response to anti-resorptive agents came from the AZURE (Does Adjuvant Zoledronic acid redUce REcurrence in stage II/III breast cancer?) trial (1). In AZURE, 3,360 women at high risk of breast cancer recurrence were randomised to receive either placebo or intensive treatment with zoledronic acid (ZOL), in addition to standard therapy, and the primary endpoint was diseases-free survival (DFS). The initial analysis that included the entire study population showed no overall increase in DFS following zoledronic acid treatment. However, sub-group analysis demonstrated that women who were postmenopausal for at least 5 years before study entry had a significantly reduced risk of DFS (25%) and the risk of death from any cause was reduced by 26%. Similar differential effects between pre- and post-menopausal patient populations have subsequently been reported from other trials, including NSABP-B34 (increased DFS in women over age 50 receiving clodronate) (2) and ABCSG-12 (increased survival in women over age 40 who receive zoledronic acid) (3). Surprisingly, these bone-targeted agents also reduced the risk of extra-skeletal recurrence, indicating that modifying the bone microenvironment affects subsequent tumour progression in distant sites.

During metastasis, the spread of breast tumour cells from the primary site to specific niches in the bone marrow is generally accepted to be an early event, and metastases may originate from these disseminated tumour cells. Once established in putative metastatic niches in bone, tumour cells can remain dormant for several years under the control of environmental cues, and in many cases never develop into clinically overt metastasis (4,5). During this period there is a close association between tumour cells and the main cell types of the bone microenvironment, bone forming osteoblast and bone resorbing osteoclasts (6). Eventually, yet to be identified events trigger the escape of tumour cells from dormancy, and initiate tumour progression and the development of overt bone metastasis. Modification of the bone microenvironment has been shown to affect the levels of tumour cell colonisation (7). Evidence from model systems demonstrated that expansion of the osteoblast niche by administration of parathyroid hormone (PTH) increased subsequent colonisation of bone by prostate cancer cells (7). The osteoclast is also key to tumour progression in bone, as pre-treatment with anti-resorptive agents inhibits subsequent breast tumour growth in bone and delays the progression of established tumours (8). To optimise tumour engraftment, the majority of xenograft models of bone metastasis use young animals (5-6 week old) with an immature skeleton and rapid bone remodelling, supporting the notion that increased osteoclast activity and/or bone turnover facilitates skeletal tumour cell colonisation and

progression. In agreement with this, studies from model systems have demonstrated that anti-resorptive agents (mainly zoledronic acid) also inhibit development of bone metastasis in young animals (9). However, the majority of patients who develop breast cancer bone metastasis will have undergone menopause, and for this group the clinical relevance of data obtained using standard xenograft models is limited. This study is the first to establish how breast tumour cells grow bone in models that mimic the pre- and post-menopausal bone microenvironment, and to demonstrate that the potent anti-resorptive agent zoledronic acid differentially modifies tumour growth in these two settings.

Materials and Methods

Cell Culture

Low passage (< P10) human breast cancer cells, MDA-MB-231-luc2 tdTomato (authenticated and purchased from Caliper Lifer Sciences, Cheshire, UK) or MDA-MB-231 (European Collection of Cell Cultures, Wiltshire, UK) transfected with eGFP were used. Prior to *in vivo* inoculation eGFP expressing cells were incubated for 15 minutes with 25μM of 1,1′-Dioctadecyl-′, 3′-Tetramethylindodicarbocyanine, 4-Chlorobenzenesulfonate (DiD) (Life Technologies, Paisley, UK). Tumour growth was monitored using an IVIS (luminol) system (Caliper Life Sciences) (luc2) or an Illumatool Lighting System (LightTools Research, Encintas, CA) (eGFP).

In vivo studies

We used 12-week-old female Balb/c nude mice (Charles River, Kent, UK). Experiments were carried out in accordance with local guidelines and with Home Office approval under project licence 40/3462, University of Sheffield, UK.

Following ovariectomy (OVX) or sham operation animals were sacrificed 1-8 weeks later (n=5/group) and bone effects assessed. Effects of OVX on tumour cell homing and colonisation of bone were established by OVX/sham operating mice 7 days before tumour cell inoculation (n=10/group). For studies of bone homing and colonisation mice were culled 24h and 8 weeks after tumour cell injection, respectively. Effects of OVX on disseminated tumour cells were assessed following injection of breast cancer cells 7 days before OVX, sham, or non-operation (n=10/group) in ER+ve and ER-ve cell lines. 1×10^5 DiD labelled MDA-MB-231-luc-2 tdTomato cells were injected into the left cardiac ventricle (i.c.), tumour growth was monitored for 8 weeks. 0.1mls saline or 1×10^5 MCF7 cells were injected i.c. 4 days following sham or implantation of 17β estradiol pellet (innovative Research of America). Effects of estradiol alone were assessed at 4 weeks and tumour growth monitored for 10 weeks.

Effects of ZOL on OVX-induced tumour growth were investigated in mice inoculated with 1×10^5 DiD labelled MDA-MB-231-eGFP cells i.c., and given weekly ZOL (100 μg/kg) or saline (n=20/group) from day 5. Seven days following tumour cell inoculation, animals from both groups underwent either sham or OVX (n=10). Assessment of PTH on tumour growth was investigated in mice inoculated with 1×10^5 MDA-MB-231-luc-2 tdTomato cells i.c.,

and given PTH (80μg/kg) or saline daily for 5 days (n=10/group) and animals sacrificed at 5 weeks.

Serum was stored at −80°C for ELISA, tibiae and femurs were fixed in 4% PFA for μCT analysis before decalcification in 1%PFA/0.5% EDTA and processing for histology. Bones for two-photon analysis were stored in OCT at −80°C.

Microcomputed tomograpgy imaging

Microcomputed tomography analysis was carried out using a Skyscan 1172 x-ray-computed microtomography scanner (Skyscan, Aartselaar, Belgium) equipped with an x-ray tube (voltage, 49kV; current, 200uA) and a 0.5-mm aluminium filter. Pixel size was set to 5.86 μm and scanning initiated from the top of the proximal tibia as previously described (10).

Bone histology and measurement of tumour volume

Osteoclasts were detected by toluidine blue and tartate-resistant acid phosphatase (TRACP) staining as previously described (11). Osteoblasts were identified as mononuclear, cuboidal cells residing in chains along the bone surface. The number of osteoclasts/osteoblasts per millimeter of cortical-endosteal bone surface and trabecular bone surfaces and the proportion of bone surface occupied by osteoclasts/osteoblasts was determined using a Leica RMRB upright microscope and OsteoMeasure software (Osteometrics inc.) as previously described (12).

Two-photon microscopy

Tibiae were imaged using a multiphoton confocal microscope (LSM510 NLO upright; Zeiss, Cambridge, UK). DiD labelled cells were visualised using a 900nm Chameleon laser, bone was detected using the 633nm multiphoton laser (Coherent, Santa Clara, CA.) and images were reconstructed in LSM software version 4.2 (Zeiss).

Biochemical analysis

Serum concentrations of TRACP 5b, P1NP and PTH were measured using commercially available ELISA kits: MouseTRAP™ Assay (Immunodiagnostic systems), Rat/Mouse P1NP competitive immunoassay kit (Immunodiagnostic Systems) and Mouse PTH (Uscn Life Sciences), respectively

Real-time PCR

Gene expression was analysed on 3 custom-made microarray plates (Ref: 0186817032) per group (all reagents from Applied Biosystems, Warrington UK): Relative mRNA expression compared with the housekeeping gene glyceraldehyde-3-phosphate dehydrogenase (GAPDH; Hs99999905_m1) was assessed using an ABI 7900 PCR System (Perkin Elmer, Foster City, CA) and Taqman universal master mix). Fold change in gene expression between treatment groups was assessed by directly inserting CT values into Data Assist V3.01 software (Applied Biosystems) and changes in gene expression were only analysed for genes with a CT value of ≤25.

Statistical Analysis

Statistical analysis was by one way analysis of variance (ANOVA) followed by Newman-Keuls multiple comparison test. Statistical significance was defined as P less than or equal to 0.05. All P values are two-sided.

Results

Characterisation of ovariectomy-induced changes in the bone microenvironment

A longitudinal study was performed to establish how OVX modified the bone microenvironment in Balb/c nude mice (figure 1). Ovariectomised animals had significantly reduced trabecular bone volume by week two, compared to sham operated animals ($p<0.01$), associated with an initial increase in the serum levels of the osteoclast marker TRACP, and corresponding decrease in the osteoblast activity marker P1NP. There was no significant difference in either osteoblast or osteoclast numbers between sham and OVX animals at any time point. In subsequent experiments tumour cells were inoculated seven days following OVX for tumour cell colonisation to coincide with bone loss. The bone microenvironment following sham or OVX was considered to model the pre- and post-menopausal setting, respectively.

Effects of ovariectomy on homing of breast tumour cells and colonisation of bone

Tumour growth in bone was investigated following i.c. injection of MDA-MB-231 breast cancer cells in female mice. In pilot studies, 90% of 6-week old animals had detectable skeletal tumour growth following this protocol (supplementary figure 1), compared to only 20% of 12-week old animals, a difference attributed to the higher rate of bone turnover in young animals.

We investigated whether the OVX-induced changes to the bone microenvironment modified the ability of breast cancer cells to home to and colonise bone. MDA-MB-231 cells were injected into 12-week old mice 7 days after OVX or sham operation. 24h after tumour cell injection flow cytometric analysis of cells flushed from the marrow cavity of long bones showed significantly higher numbers of tumour cells in control mice compared with OVX animals (427.7 ± 87.6 tumour cells/1×10^6 mononuclear in control v.s. 150.7 ± 23.17 in OVX mice ($P<0.005$) (supplementary figure 2a), implying that OVX decreases the initial number of tumour cells that home to the bone microenvironment. Multiphoton analysis of the bones confirmed these results (supplementary fig 2b). 48 days following tumour cell injection tumour growth in bone was detected in 17% of control and 18% of sham operated animals, compared to 89% of animals that had undergone OVX ($p<0.001$ for OVX vs. control or sham, figure 2). Number and size of tumours in the long bones were increased following OVX, with 1.67 ± 0.41 tumours detected per mouse with an average BIL of $1.09\times10^6 \pm 0.09\times10^6$ photons per second (p/s) following OVX compared with 0.43 ± 0.12 tumours with an average BIL of $0.23\times10^6 \pm 0.08\times10^6$ p/s following sham operation ($P<0.001$). Tumour burden in non-bone sites was similar in all groups (18% in OVX, 17% in control and 18% in sham). OVX induced the expected reduction in bone volume compared to sham/control (BV/TV = 9.11 ± 0.32% in OVX, 13.85 ± 0.23% in control and 14.07 ± 0.13% in sham; $p<0.001$ for OVX vs. control or sham), supporting that modification of the

bone microenvironment is associated with increased tumour cell colonisation and/or ability of tumour cells to form overt colonies.

Effects of ovariectomy on growth of disseminated breast tumour cells in bone

Following i.c. implantation of MDA-MB-231 cells in 12-week old animals, the majority of tumour cells that reach bone die within 72h, leaving behind a small number of disseminated tumour cells that do not form overt colonies. We investigated whether modifying the bone microenvironment through OVX affects the ability of these disseminated tumour cells to form colonies. OVX performed seven days following tumour cell injection resulted in a substantial increase in tumour growth in bone, accompanied by a 34% and 36% loss in trabecular bone compared to the sham or control group respectively ($P<0.001$) (figure 3). 89 % of animals that had undergone OVX developed tumours in bone, compared to 17% of the animals in the control and 11% in the sham group ($P<0.001$ for OVX vs. control or sham). Compared to the sham group, animals in the OVX group had both increased number (2.55 ± 0.86 tumours per long bone vs. 0.46 ± 0.32) and larger tumours (1.35×10^6 ± 0.02 p/s vs. 0.02 ± 0.01 p/s). The OVX-induced increase in tumour growth was specific to bone, with extra-skeletal tumours detected in 18% of OVX, 17% of control and 18% of sham operated animals.

Differential effects of osteoclast inhibition on tumour growth in bone in the pre- and post-menopausal setting

We investigated whether tumour growth in bone was driven by increased bone resorption by treating sham and OVX animals with the potent osteoclast inhibitor ZOL. MDA-MB-231 cells were injected i.c. in two groups of animals that received weekly injections of saline (control, n=20) or ZOL (100ug/kg, n=20) for 4 weeks. Half of the animals from each group subsequently underwent either a sham operation or OVX on day 7 (n=10/group) and tumour growth was monitored until day 35. 86% animals that underwent OVX had detectable tumours in bone compared to 33% of sham ($P<0.001$), supporting that increased bone resorption stimulated tumour growth in the post-menopausal setting (figure 4). There was a significant reduction of tumour growth in bone in OVX animals treated with ZOL (17%) compared to OVX control (86%) ($P<0.001$). In contrast, ZOL treatment did not affect skeletal tumour growth in the sham group, with 33% of both control and ZOL treated sham operated animals having detectable tumours in bone. Despite the differential effects on tumour growth, ZOL caused a significant increase in bone volume in both OVX and sham operated animals compared to the respective controls (figure 4 c-d). Bone volume/trabecular volume increased from 12.91 ± 1.25% in sham OVX to 17.21 ± 1.15% in sham ZOL ($p<0.01$) and from 10.52 ± 1.29% in OVX control compared with 16.25 ± 1.37% ($P<0.01$), no significant differences in bone volume were detected between sham or OVX animals treated with ZOL, demonstrating that bone resorption is reduced to the same extent in models of pre- and post-menopausal bone.

Multiphoton microscopy confirmed the presence of individual MDA-MB-231 cells in the long bones of animals that had not developed overt bone tumours on day 35 regardless of group, demonstrating that the tumour cells successfully engrafted in bone but remained non-proliferative for extensive periods in all settings (figure 5).

OVX-induced gene expression changes in the bone microenvironment are modified by ZOL

We compared the expression of a panel of genes using long bones isolated from control and ZOL treated animals seven days following OVX or sham operation. The genes were selected based on reported roles in bone turnover and/or tumour growth in bone, as well as stem cell mobilisation. Table 1 shows the genes for which a more than two-fold change in expression levels between OVX and sham was detected. A full gene list is given in supplementary table 2. As expected, OVX induced expression of a number of genes associated with increased bone resorption (including Cathepsin K, TRAP, MMP9, RANKL and PTH), which was inhibited by treatment with ZOL. There was a significant change in genes affecting bone formation following OVX (including reduced expression of the osteoblast formation inhibitors Dkk1, 2 and 3), and this was reversed in the ZOL treated animals. ZOL modified expression genes linked to bone turnover in both the sham and OVX animals, in agreement with the ability of ZOL to inhibit bone loss in both groups (figure 4). Interestingly, ZOL differentially modified genes associated with stem cell mobilisation in sham and OVX animals.

Effects of PTH on MDA-MB-231 tumour growth in bone

Molecular analysis of bones from OVX operated animals showed a significant increase in PTH expression compared with sham operated animals, which was reversed by treatment with ZOL. Analysis of serum from OVX and sham operated animals by ELISA showed a trend towards increased levels of PTH following OVX (12.82 ± 1.12 pg/ml) compared with control (16.31 ± 1.25) although this did not reach significance ($P = 0.055$, data not shown). We therefore investigated the effects of PTH on tumour growth in bone. Administration of 80μg/kg rhPTH for 5 days resulted in a 29% increase in TRAP levels reflecting elevated osteoclast activity, accompanied by an increase in tumours from 0.6/mouse in control to 2.14/mouse in PTH treated animals (supplementary figure 3a and b). These data demonstrate a correlation between increased bone resorption and tumour growth in bone, similar to those obtained following OVX.

Discussion

Using experimental systems that separately model the pre- and post-menopausal bone microenvironment, combined with advanced imaging of disseminated tumour cells in bone, we have identified major differences in tumour growth and response to anti-resorptive therapy. Breast cancer cells homed to the long bones following intra-cardiac inoculation in 12-week old mice, but failed to progress to form overt tumours in the majority of animals unless preceded by OVX (Figure 2). OVX also induced the growth of disseminated tumour cells in bone, whereas a sham operation did not (Figure 3). We used the established oestrogen-independent MDA-MB-231 cells, as oestrogen-dependent MCF7 cells did not form bone metastasis following i.c. injection 10 weeks after implantation (data not shown). Oestrogen supplementation caused major changes to the bone volume structure significantly altering the bone microenvironment and hence was unsuitable for our studies (supplementary figure 4).

A limitation of our study is the differences in bone turnover rates in mice and humans, with changes to the bone microenvironment following OVX manifesting themselves within a few days in mice. These rapid changes may affect the growth of resident tumour cells to a higher degree than would be the case in humans. However, as early stages of tumour cell colonisation of bone cannot be studied in patients, model systems continue to provide valuable information relating to initiation of bone metastasis. ZOL specifically inhibited OVX-induced bone tumour growth, supporting the observed benefit of anti-resorptive therapy in post-menopausal breast cancer patients (1, 3). In contrast, no effect on tumour growth in bone was seen in sham operated animals, reflecting the lack of benefit of adjuvant ZOL in the pre-menopausal breast cancer patients (1, 13). Our results provide new insights into the mechanisms driving tumour growth in bone that may contribute to differential therapeutic effects of ZOL in the pre-and post-menopausal setting.

We present two major findings; firstly, that OVX-induced changes to the bone microenvironment can trigger growth of disseminated breast tumour cells, and secondly, that these changes are completely abolished by ZOL and hence mediated by osteoclast activity. Our data support that tumour cells remain quiescent in the mature skeleton until they receive microenvironmental signals that stimulate their proliferation. Tumour cells that persist in bone are thought to occupy specific niches identical to, the hematopoietic stem cell (HSC) niche (7). Tumour proliferation in bone may therefore be regulated by many of the same processes that control HSC mobilisation and quiescence, including osteoblast and osteoclast activities (14-16). Although not clearly defined, the “bone metastatic niche” maybe located at endosteal bone surfaces in the long bones. In agreement, the single tumour cells we detected in bone were closely associated with endosteal surfaces of trabecular bone in proximity to the growth plate (figure 5).

There is accumulating evidence that osteoclasts are central to mobilisation of HSCs, mainly through the production of proteolytic enzymes that disrupt SDF-1-CXCR4 interactions (14). Increased bone resorption following administration of RANKL stimulates egress of HSCs from bone marrow niches into the circulation, disrupts the adhesion of HSCs and niche components that maintain cell quiescence resulting in proliferation (17). Other ‘stress’ signals in the endosteal niche, e.g. OVX-induced bone loss, may have similar effects. Remodelling of the extracellular matrix during bone resorption may also disrupt integrin interactions that maintain tumour cells in a state of quiescence (18).

Previous studies addressing the long-term skeletal effects of OVX in mouse models, show significant bone loss persisting for several weeks (19-20). To capture the events associated with induction of disseminated tumour cell proliferation, we investigated the molecular and cellular changes to the bone microenvironment seven days after OVX/sham operations. At this point, a range of genetic changes reflecting increased bone resorption and/or reduced bone formation were detectable (table 1). OVX induced a significant increase in expression of RANKL, a stimulator of osteoclast formation and activity (21), coupled with decreased expression of the RANKL inhibitor osteoprotegerin (22). In addition, Dkk-1, an inhibitor of osteoblast differentiation was increased (23). OVX also caused increased expression of proteolytic enzymes associated with elevated osteoclast activity, including MMP-9 and Cathepsin K (24). In addition to the established roles in bone turnover, these molecules also

activate the bone marrow endosteal stem cell niche and stimulate mobilisation of vasculogenic progenitors (25). MMP9 plays a critical role in mobilisation of hematopoietic and endothelial precursor cells from the bone marrow niche through cleaving of membrane KitL to its soluble form, a key component of the osteoblast stem cell niche essential for endosteal lodging of murine stem cells (24). Interestingly, c-KitL was the gene most upregulated following OVX. It is possible that changes in the levels of cKitL may also affect the mobilisation of tumour cells that reside in the niche. We hypothesise that the non-proliferating tumour cells present in the bone marrow prior to OVX are the cells that have the capacity to form tumours and hence have stem cell like properties, and modification of the bone microenvironment mediates mobilisation of these cells from bone marrow niches and initiate tumour growth. Importantly, the increased tumour growth following OVX was not a result of increased numbers of tumour cells homing to bone compared to sham (supplementary figure 2).

We used the anti-resorptive agent, ZOL, to establish whether OVX-induced tumour growth was triggered by increased osteoclast activity. ZOL increased bone volume to the same extent in animals that had undergone either sham or OVX, reflected by changes in bone gene expression levels. These results are in agreement with clinical studies showing that ZOL decreases the level of bone resorption markers in both pre- and post-menopausal women (1, 13). However, we found major differences in the ability of ZOL to modify tumour growth in bone. In the sham group, mimicking the pre-menopausal setting, ZOL had no effect on the growth of skeletal tumours (figure 4). In contrast, ZOL completely prevented OVX-induced tumour growth in bone (mimicking the post-menopausal setting). Only four genes (KitL, Igf1, Igf2 and MmP14) in our panel were differentially affected by ZOL in the OVX vs. the sham group, all of which are associated with regulating stem cell niches (26-28). Further studies are required to establish the role of these changes in initiation of bone metastasis. Tumour growth outside the skeleton (including lung) was not affected by ZOL treatment in either group, but the models do not capture metastasis to extra-skeletal sites that may occur during subsequent tumour progression. We have previously shown that administration of 100ug/kg ZOL weekly for 6 weeks does not induce tumour cell apoptosis in a bone metastasis model, hence ZOL does not reduce tumour growth by direct tumour cell toxicity (29). There are clear limitations to mimicking effects of menopause in mice, in particular the role of the changes in circulating hormones. However, our results clearly indicate that breast tumour progression in bone involves different mechanisms in the pre- and post-menopausal microenvironment, and that it may potentially only be driven by osteoclast activity in post-menopausal bone.

Our data are the first to demonstrate that the cellular and molecular mechanisms are responsible for driving tumour growth differ in the pre- (sham) and post-menopausal (OVX) bone metastasis models. We show that osteoclast-mediated mechanisms are instrumental for the progression of disseminated tumour cells in bone only in the post-menopausal model, and hence provide biological evidence underpinning why the benefit of adjuvant anti-resorptive therapy reported is restricted to post-menopausal breast cancer patients in recent clinical trials.

Supplementary Material

Refer to Web version on PubMed Central for supplementary material.

Acknowledgments

We are grateful for the support from Miss Orla Gallagher and Mr Darren Lath who provided expert bone processing and sectioning. This study was supported by a program grant from Cancer Research UK (to CLE, PIC and IH). PIC is supported by Mrs Janice Gibson and the Ernest Heine Family Foundation.

References

1. Coleman RE, Marshall H, Cameron D, Dodwell D, Burkinshaw R, Keane M, et al. Breast cancer adjuvant therapy with zoledronic acid. New England Journal of Medicine. 2011; 365:1396–405. [PubMed: 21995387]
2. Paterson AHG, Anderson SJ, Lembersky BC, Fehrenbacher L, Falkson CI, King KM, et al. S2-3: NSABP Protocol B-34: A clinical trial comparing adjuvant clodronate vs. placebo in early stage breast cancer patients receiving systemic chemotherapy and/or tamoxifen or no therapy – final analysis. Cancer Research. 2011; 71(24 Suppl 3):S2–3.
3. Gnant M, Mlineritsch B, Stoeger H, Luschin-Ebengreuth G, Heck D, Menzel C, et al. Adjuvant endocrine therapy plus zoledronic acid in premenopausal women with early-stage breast cancer: 62-month follow-up from the ABCSG-12 randomised trial. Lancet Oncol. 2011; 12:631–41. [PubMed: 21641868]
4. Townson JL, Chambers AF. Dormancy of solitary metastatic cells. Cell Cycle. 2006; 16:1744–50. [PubMed: 16861927]
5. Aguirre-Ghiso JA. Models, mechanisms and evidence for cancer dormancy. Nature Reviews Cancer. 2007; 7:834–846.
6. Weilbaecher KN, Guise TA, McCauley L. Cancer to bone: a fatal attraction. Nature Reviews Cancer. 2011; 11:411–25.
7. Shiosawa Y, Pedersen EA, Havens AM, Jung Y, Mishra A, Joseph J, et al. Human prostate cancer metastases target the hematopoietic stem cell niche to establish footholds in mouse bone marrow. J Clin Invest. 2011; 121:1298–1312. [PubMed: 21436587]
8. van der Pluijm G, Que I, Sijmons B, Buijs JT, Löwik CW, Wetterwald A, et al. Interference with the microenvironmental support impairs the de novo formation of bone metastases in vivo. Cancer Res. 2005; 65:7682–90. [PubMed: 16140935]
9. Brown HK, Holen I. Anti-tumour effects of bisphosphonates – what have we learned from in vivo models? Current Cancer Drug Targets. 2009; 9:807–23. [PubMed: 20025569]
10. Ottewell PD, Mönkkönen H, Jones M, Lefley DV, Coleman RE, Holen I. Antitumor effects of doxorubicin followed by zoledronic acid in a mouse model of breast cancer. J Natl Cancer Inst. 2008; 100:1167–78. [PubMed: 18695136]
11. Cole AA, Walters LM. Tartrate-resistant acid phosphatase in bone and cartilage following decalcification and cold-embedding in plastic. J Histochem Cytochem. 1987; 35:203–6. [PubMed: 3540104]
12. Parfitt AM, Drezner MK, Glorieux FH, Kanis JA, Malluche H, Meunier PJ, et al. Report of the ASBMR Histomorphometry Nomenclature Committee. Bone histomorphometry: standardization of nomenclature, symbols, and units. J Bone Miner Res. 1987; 2:595–610. [PubMed: 3455637]
13. Steinman EA, Brufsky AM, Oesterreich S. Zoledronic acid effectiveness against breast cancer metastases – a role for oestrogen in the microenvironment? Breast Cancer Research. 2012; 14:213. [PubMed: 23014660]
14. Kollet O, Dar A, Lapidot T. The multiple roles of osteoclasts in host defence: Bone remodelling and hematopoietic stem cell mobilisation. Annu Rev Immunol. 2007; 25:51–69. [PubMed: 17042735]
15. Renstrom J, Kroger M, Peschel C, Oostendorp RAJ. How the niche regulates hematopoietic stem cells. Chemico-Biological Interactions. 2010; 184:7–15. [PubMed: 19944675]

16. Ellis SL, Grassinger J, Jones A, Borg J, Camenisch T, Haylock D, et al. The relationship between bone, hemopoietic stem cells and vasculature. Blood. 2011; 118:1516–1524. [PubMed: 21673348]
17. Kollet O, Dar A, Shivtiel S, Kalinkovich A, Lapid K, Sztainberg Y, Tesio M, et al. Osteoclasts degrade endosteal components and promote mobilisation of hematopoietic progenitor cells. Nature Medicine. 2006; 12:657–64.
18. Barkan D, Green JE, Chambers AF. Extracellular matrix: a gatekeeper in the transition from dormancy to metastatic growth. Eur J Cancer. 2010; 46:1181–8. [PubMed: 20304630]
19. Lee SK, Kadono Y, Okada F, Jacquin C, Koczon-Jaremko B, Gronowicz G, Adams DJ, et al. T lymphocyte-deficient mice lose trabecular bone mass with ovariectomy. J Bone Miner Res. 2006; 21:1704–12. [PubMed: 17002560]
20. Orlić I, Borovecki F, Simić P, Vukicević S. Gene expression profiling in bone tissue of osteoporotic mice. Arh Hig Rada Toksikol. 2007; 58:3–11. [PubMed: 17424779]
21. Lacey DL, Timms E, Tan HL, Kelley MJ, Dunstan CR, Burgess T, et al. Osteoprotegerin ligand is a cytokine that regulates osteoclast differentiation and activation. Cell. 1998; 93:165–76. [PubMed: 9568710]
22. Simonet WS, Lacey DL, Dunstan CR, Kelley M, Chang MS, Lüthy R, et al. Osteoprotegerin: a novel secreted protein involved in the regulation of bone density. Cell. 1997; 89:309–19. [PubMed: 9108485]
23. van der Horst G, van der Werf SM, Farih-Sips H, van Bezooijen RL, Löwik CW, Karperien M. Downregulation of Wnt Signalling by increased expression of Dickkopf-1 and -2 is a prerequisite for late stage osteoblast differentiation of KS483 cells. J Bone Mineral Res. 2005; 20:1867–77.
24. Jodele S, Blavier L, Yoon JM, DeClerck YA. Modifying the soli to affect the seed: role of stromal-derived matrix metalloproteinases in cancer progression. Cancer Metastasis Rev. 2006; 25:35–43. [PubMed: 16680570]
25. Aicher A, Kollet O, Heeschen C, Liebner S, Urbich C, Ihling C, et al. the Wnta antagonist Dickkopf-1 mobilises vasculogenic progenitor cells via activation of the bone marrow enodstal stem cell niche. Circ Res. 2008; 103:796–803. [PubMed: 18776043]
26. Driessen RL, Johnston HM, Nilsson SK. Membrane bound stem cell factor is a key regulator in the initial lodgement of stem cells within the endosteal marrow region. Experimental Hematology. 2003; 31:1284–91. [PubMed: 14662336]
27. Kumar S, Ponnazhagan S. Mobilization of bone marrow mesenchymal stem cells in vivo augments bone healing in a mouse model of segmental bone defect. Bone. 2012; 50:1012–8. [PubMed: 22342795]
28. Lu C, Li XY, Hu Y, Rowe RG, Weiss SJ. MT1-MMP controls human mesenchymal stem cell trafficking and differentiation. Blood. 2010; 115:221–229. [PubMed: 19901267]
29. Ottewell PD, Woodward JK, Lefley DV, Evans CA, Coleman RE, Holen I. Anticancer mechanisms of doxorubicin and zoledronic acid in breast cancer tumor growth in bone. Mol Cancer Ther. 2009; 8:2821–32. [PubMed: 19789217]

Europe PMC Funders Author Manuscripts

Europe PMC Funders Author Manuscripts

Statement of translational relevance

Our study addresses the surprising findings from clinical trials that addition of zoledronic acid to standard chemotherapy and/or hormone therapy has differential effects depending on the patients' menopausal status, with the survival benefits being restricted to patients with established menopause. Our study provides the first comprehensive in vivo evidence of how the cellular mechanisms involved in initiating bone metastasis differ in the pre- and post menopausal bone microenvironment. Our data also demonstrate a link between menopausal status and the differential anti-tumour effects of zoledronic acid. We show that osteoclast-mediated mechanisms are instrumental in the tumourigenic progression of disseminated breast cancer cells in bone exclusively in the post-menopausal setting; providing the biological evidence that support specific benefits of adjuvant anti-resorptive therapy for post-menopausal breast cancer patients.

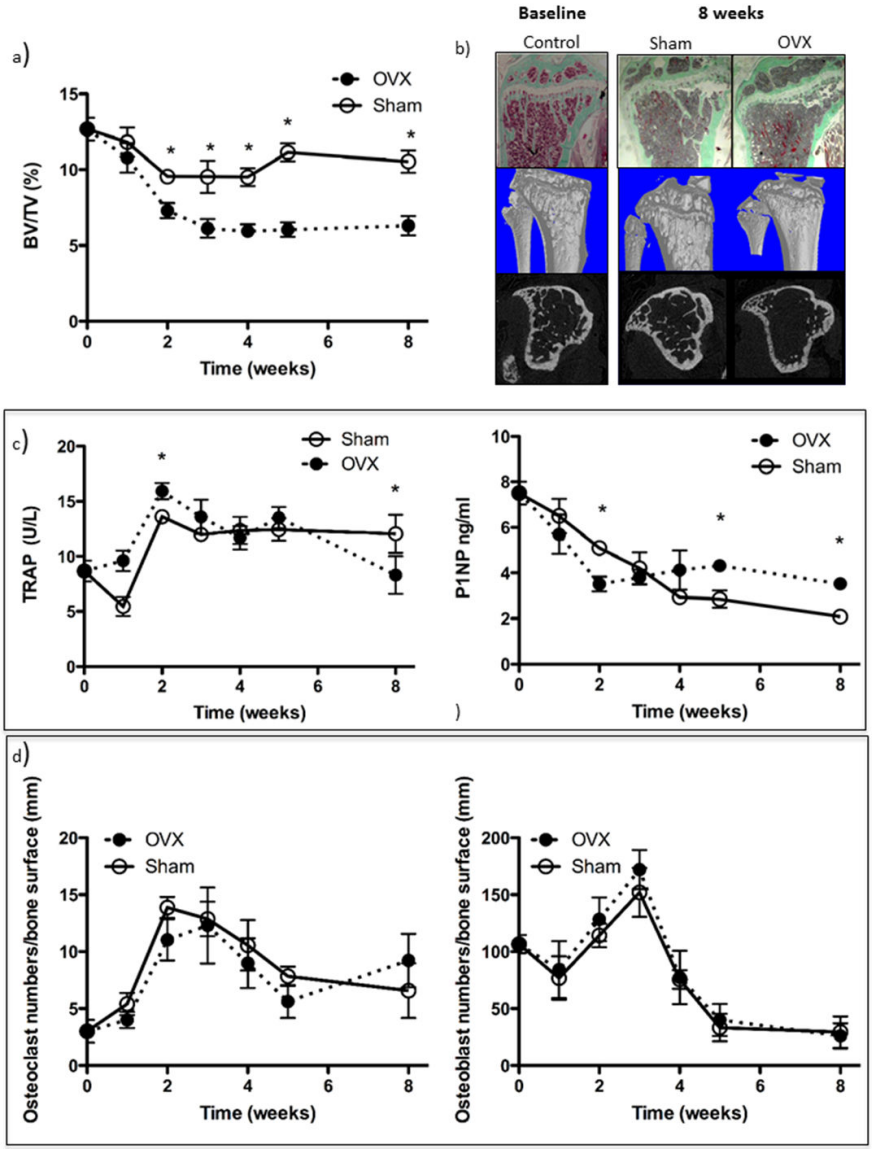

Figure 1. Effects of ovariectomy on bone structure and bone turnover

(a) Bone volume 0, 1, 2, 3, 4, 5 and 8 weeks following ovariectomy. **(b)** Photomicrographs of Goldners' stained histological sections of the tibia and reconstructed μCT images at baseline and 8 weeks following ovariectomy or sham operation. Osteoclast activity was analysed by measuring serum levels of TRACP 5b and osteoblast activity assessed by measuring P1NP **(c)** in ovariectomised mice compared with sham operated animals. Numbers of osteoclasts and osteoblasts **(d)** lining the bone surface 0, 1, 2, 3, 4, 5 and 8 weeks following ovariectomy. Data shown are mean ± SEM and * represents a p value of < 0.05.

Europe PMC Funders Author Manuscripts

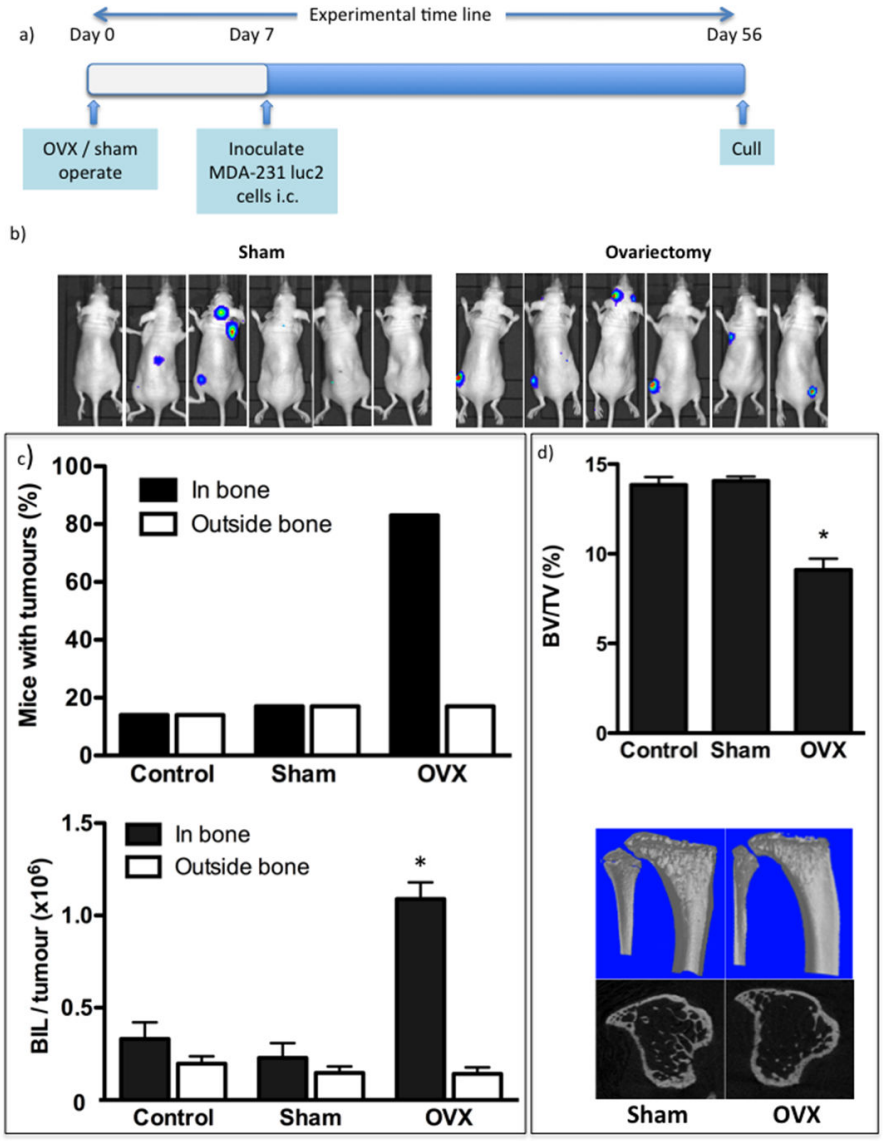

Figure 2. Ovariectomy increases of the number of MDA-MB-231 breast cancer cell colonies in bone

Experimental outline **(a)** and **(b)** photographs of luciferase expressing MDA-MB-231 cells inoculated 7 days after ovariectomy or sham operation and 56 days following tumour cell inoculation. The percentage of mice with detectable tumours and mean tumour volume ± SEM shown as numbers of photons per second per tumour **(c)**. Bone volume following ovariectomy in mice injected with MDA-MB-231 cells (mean ± SEM) and uCT images representing bone architecture **(d)**. All data are shown for 56 days following tumour cell inoculation and * represents a p value of < 0.05.

Europe PMC Funders Author Manuscripts

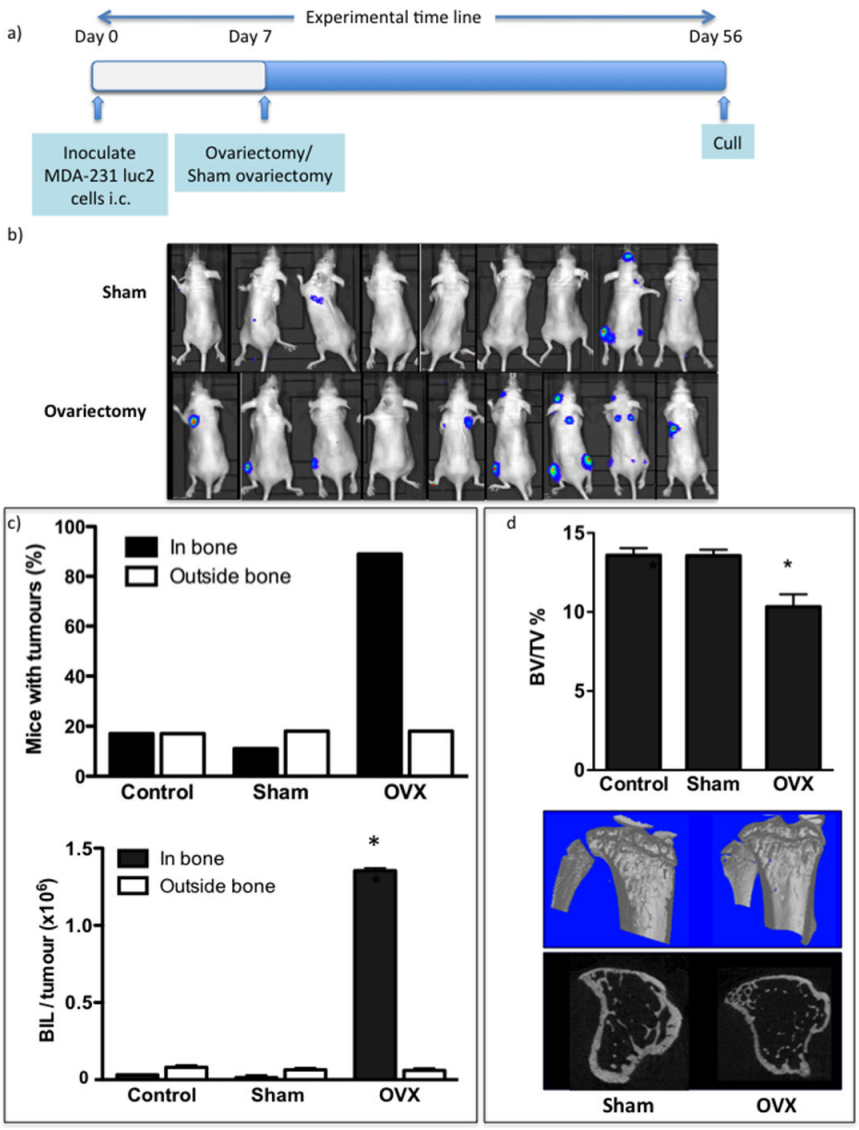

Figure 3. Ovariectomy stimulates growth of established breast cancer cells in long bones of 12-week-old immunocompromised mice

Experimental outline **(a)** and photographs of luciferase expressing MDA-MB-231 cells inoculated 7 days before ovariectomy or sham operation growing in mice 49 days following tumour cell inoculation **(b)**. Percentage of mice with detectable tumours and mean tumour volume ± SEM is shown as numbers of photons per second per tumour **(c)**. Effects on bone volume following ovariectomy in mice injected with MDA-MB-231 cells (mean ± SEM) and μCT images representing bone architecture **(d)**. All data are shown for 49 days following tumour cell inoculation and * represents a p value of < 0.05.

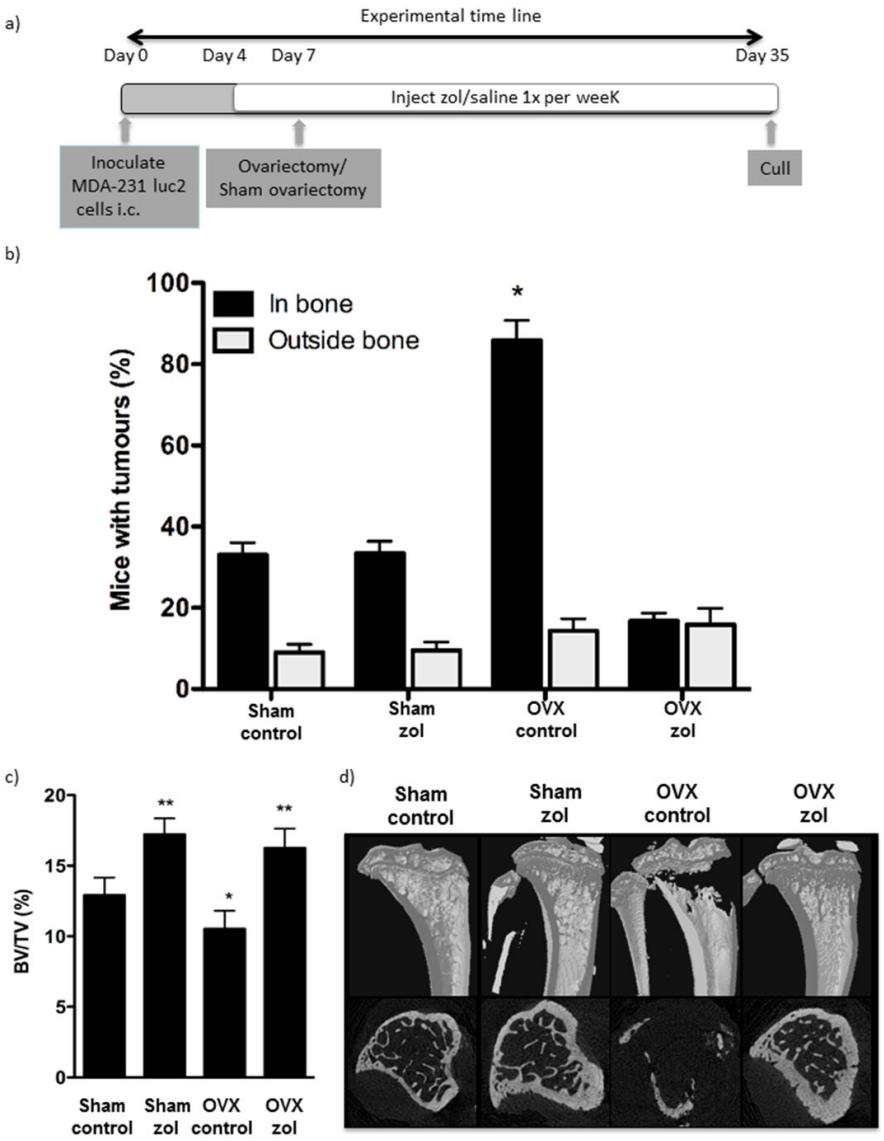

Figure 4. Zoledronic acid inhibits bone resorption and reduces tumour take in ovariectomised mice

(a) Experimental outline. **(b)** Histogram showing mean ± SEM % of mice with detectable bone tumours in control and zoledronic acid treated ovariectomised and sham operated mice 35 days following tumour cell inoculation. **(c)** Bone volume compared with trabecular volume 28 days following ovariectomy and 31 days following zoledronic acid treatment in mice pre-injected with MDA-MB-231 cells (mean ± SEM). **(d)** μCT images representing bone architecture at the end of the experimental protocol. * represents a p value of < 0.05 compared with sham control and ** a p value of < 0.05 compared with sham control and OVX control.

Europe PMC Funders Author Manuscripts

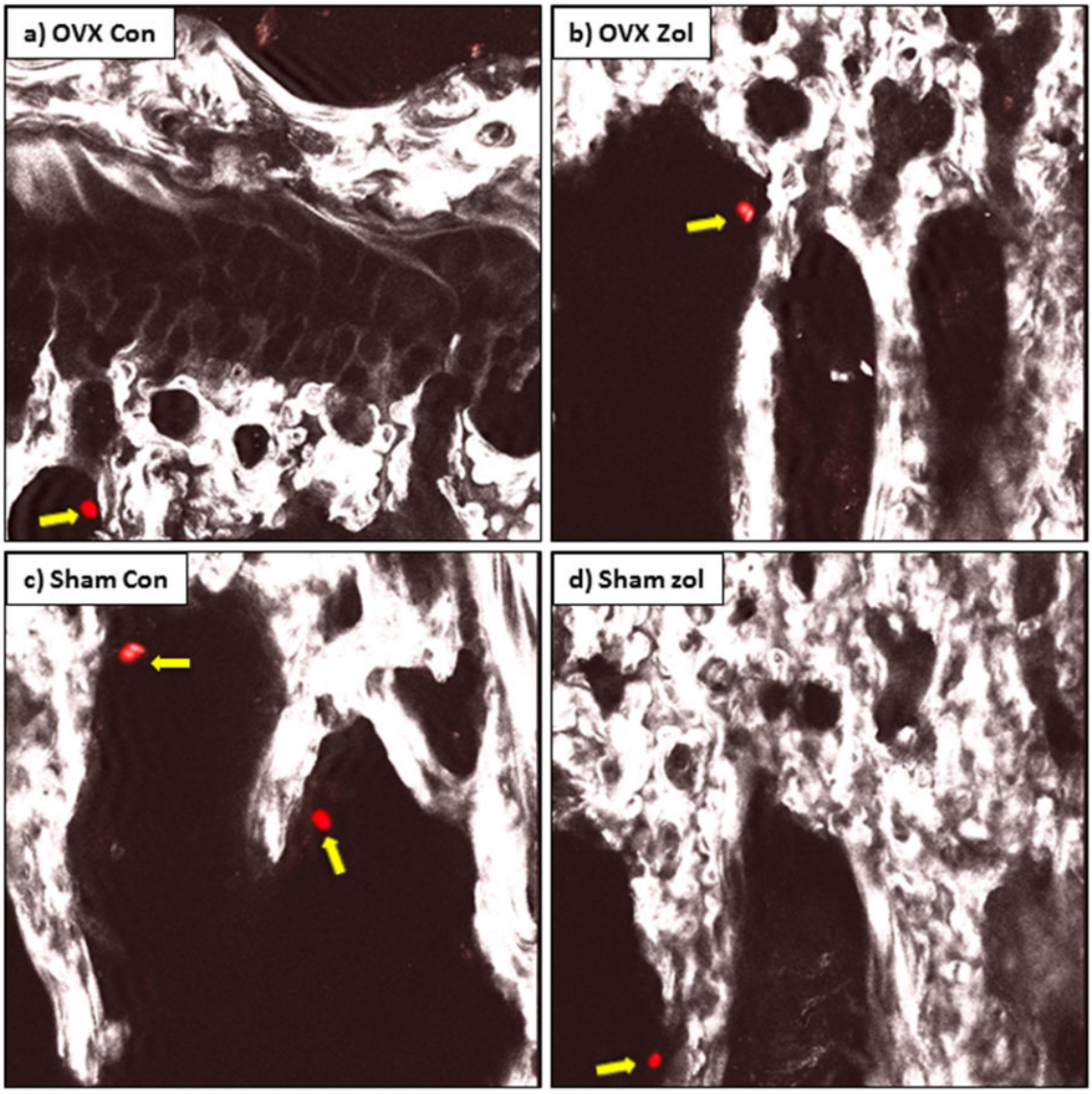

Figure 5. Non-proliferating tumour cells are present in proximal trabecular bone of mice without detectable metastasis

Confocal images of disseminated DiD labelled tumour cells (red cells highlighted with yellow block arrows) that have homed to bone but not formed tumours in tibiae of ovariectomised control mice **(a)**, ovariectomised zoledronic acid treated mice **(b)**, sham control **(c)** and sham zoledronic acid treated animals **(d)**.

Table 1

Genetic alterations in mouse long bone 1 week following ovariectomy with and without zoledronic acid treatment

	Protein coded for	Fold Change OVX vs Sham	Fold Change Sham Zol vs Sham	Fold Change OVX Zol vs Sham Zol	Fold Change OVX Zol vs OVX
KitL	C-kit ligand	5.33 ± 0.91*	−1.34 ±1.56	4.23 ± 0.83*	− 1.90 ± 0.11
Tnfsf11	Receptor activator of nuclear factor kappa-B ligand	4.87 ± 0.58*	−2.2 ± 0.12*	0.35 ± 0.97	−6.73 ± 1.26*
BGlap	Osteocalcin	4.69 ± 2.39*	4.96 ± 1.54*	5.83 ± 0.49*	5.74 ± 2.04*
Ctsk	Cathepsin K	3.81 ± 0.12*	−3.09 ± 0.63*	0.07 ± 0.23	−6.82 ± 0.38*
Spp1	Osteopontin	3.74 ± 0.51*	−2.06 ± 0.38	0.07 ± 0.44	−5.74 ± 0.52 *
Dkk1	Dickkopf	1 3.73 ± 0.69*	−2.86 ± 0.62*	0.18 ± 0.49	−6.42 ± 0.33 *
Igf2	Insulin-like growth factor 2	3.71 ± 0.45*	0.36 ± 1.82	3.54 ± 1.36*	−0.07 ± 0.66
MmP9	Matrix metallopeptidase 9	3.54 ± 0.41*	−2.11 ± 0.22	0.24 ± 0.11	−5.40 ± 0.22*
Lif	Leukemia inhibitory factor	3.36 ± 0.54*	1.06 ± 1.15	2.22 ± 0.31*	− 0.36 ± 0.72
Cxcl12	Chemokine ligand 12	2.97 ± 0.73*	−1.65 ± 0.86	0.30 ± 0.19	−6.23 ± 1.51 *
Dkk2	Dickkopf 2	2.96 ± 0.26*	−2.60 ± 0. 42*	0.27 ± 1.02	−5.30 ± 0.42*
Sp7	Osterix	2.91 ± 0.44*	0.18 ± 0.23	2.95 ± 0.98	0.22 ± 0.09
Igf1	Insulin-like growth factor 1	2.81 ± 0.25*	0.28 ± 0.43	2.39 ± 0.26*	−0.14 ± 0.19
MmP14	Matrix metallopeptidase 14	−2.77 ± 0.23*	−0.89 ± 0.71	−2.50 ± 0.41*	−0.61 ± 0.10
Tnf	Tumour necrosis factor	2.73 ± 0.16*	−2.57 ± 0.51*	0.37 ± 0.68	−4.91 ± 0.40*
Tnfrsf11b	Osteoprotegrin	−2.56 ± 0.11*	2.87 ± 0.53*	−0.44 ± 0.51	5.00 ± 0.72*
Dkk3	Dickkopf 3	2.46 ± 0.36*	−0.58 ± 0.64	0.08 ± 0.65	−3.99 ± 0.51*
MmP2	Matrix metallopeptidase 2	−2.35 ± 0.19*	2.72 ± 0.29*	−0.17 ± 0.35	4.90 ± 0.16*
Ccnd1	Cyclin D1	−2.31 ± 0.41*	−4.13 ± 0.56*	−0.38 ± 0.52	−4.51 ± 0.72*
Pth	Parathyroid hormone	2.26 ± 0.26*	0.09 ± 0.87	−0.61 ± 0.71	−3.68 ± 1.57*
Apc5	TRAP	2.25 ± 0.22*	−2.43 ± 0.25*	0.15 ± 0.26	−5.13 ± 0.25*

* Represents a p value of < 0.05.